GABAergic inhibition of leg motoneurons is required for normal walking behavior in freely moving *Drosophila*

Swetha B. M. Gowda[a,b,1], Pushkar D. Paranjpe[a,1], O. Venkateswara Reddy[a], Devasena Thiagarajan[a], Sudhir Palliyil[a], Heinrich Reichert[c], and K. VijayRaghavan[a,2]

[a]National Centre for Biological Sciences, Tata Institute of Fundamental Research, 560065 Bangalore, India; [b]Manipal Academy of Higher Education, Manipal, 576104 Karnataka, India; and [c]Biozentrum, University of Basel, 4001 Basel, Switzerland

Contributed by K. VijayRaghavan, January 22, 2018 (sent for review August 7, 2017; reviewed by Spyros Artavanis-Tsakonas and Chun-Fang Wu)

Walking is a complex rhythmic locomotor behavior generated by sequential and periodical contraction of muscles essential for coordinated control of movements of legs and leg joints. Studies of walking in vertebrates and invertebrates have revealed that premotor neural circuitry generates a basic rhythmic pattern that is sculpted by sensory feedback and ultimately controls the amplitude and phase of the motor output to leg muscles. However, the identity and functional roles of the premotor interneurons that directly control leg motoneuron activity are poorly understood. Here we take advantage of the powerful genetic methodology available in *Drosophila* to investigate the role of premotor inhibition in walking by genetically suppressing inhibitory input to leg motoneurons. For this, we have developed an algorithm for automated analysis of leg motion to characterize the walking parameters of wild-type flies from high-speed video recordings. Further, we use genetic reagents for targeted RNAi knockdown of inhibitory neurotransmitter receptors in leg motoneurons together with quantitative analysis of resulting changes in leg movement parameters in freely walking *Drosophila*. Our findings indicate that targeted down-regulation of the $GABA_A$ receptor Rdl (Resistance to Dieldrin) in leg motoneurons results in a dramatic reduction of walking speed and step length without the loss of general leg coordination during locomotion. Genetically restricting the knockdown to the adult stage and subsets of motoneurons yields qualitatively identical results. Taken together, these findings identify GABAergic premotor inhibition of motoneurons as an important determinant of correctly coordinated leg movements and speed of walking in freely behaving *Drosophila*.

walking | premotor inhibition | interneurons | leg motoneurons | speed

Walking is a complex rhythmic locomotor behavior that requires the coordinated control of movements among legs, leg segments, and leg joints (1–5). While the complete neural circuitry of the motor control networks that orchestrate this control is not known in any animal, significant progress has been made in understanding the general organization of the underlying networks. Studies of reduced preparations in vertebrates have revealed that premotor interneuronal circuits present in the spinal cord are capable of generating patterned rhythmic locomotor activity and distributing this activity to motoneurons (6–8). Furthermore, in several cases, the function of identified spinal interneuron types in this type of fictive locomotion has been elucidated (9, 10). However, the complexity and the difficulty of genetic intervention in vertebrate models have made the cellular identification and functional analysis of these premotor control circuits difficult.

Invertebrate models have reduced complexity and for some of them, such as *Drosophila*, genetic reagents that enable visualization and perturbation of neural circuitry are available (11–13). In *Drosophila*, the neural connectivity of leg motoneurons, their structural organization, and their relationship with leg muscles has been well established (14–17). Moreover, extensive neurogenetic analyses of walking behavior in *Drosophila* have shown that higher brain centers such as the central complex, the ellipsoid body, and the mushroom bodies affect higher order phenomenon such as the drive to walk, ability to maintain a fixed course, or goal-directed locomotion (18–20). However, these central brain structures are entirely dispensable for the more mundane aspect of walking, maintaining all of the moving parts in harmony with each other. The observation that headless flies can walk demonstrates that the higher order brain regions have less contribution for coordination of leg motion and that the minimal circuitry required for the generation of rhythmic walking behavior resides in the ventral nerve cord (VNC) (21, 22). Thus, as in other insects, premotor neural circuitry in the VNC is thought to generate a basic rhythm, which is sculpted by bilateral and intersegmental coordination processes and modified by sensory feedback such that it ultimately controls the magnitude and timing of patterned motoneuronal output to leg muscles as the animal walks (23–26).

Inhibitory interactions are important features of the neural circuitry that generates walking (27–29). Inhibition is involved in

Significance

Inhibition is an important feature of the neuronal circuit, and in walking, it aids in controlling coordinated movement of legs, leg segments, and joints. Recent studies in *Drosophila* report the role of premotor inhibitory interneurons in regulation of larval locomotion. However, in adult walking, the identity and function of premotor interneurons are poorly understood. Here, we use genetic methods for targeted knockdown of inhibitory neurotransmitter receptors in leg motoneurons, combined with automated video recording methods we have developed for quantitative analysis of fly leg movements and walking parameters, to reveal the resulting slower walking speed and defects in walking parameters. Our results indicate that GABAergic premotor inhibition to leg motoneurons is required to control the normal walking behavior in adult *Drosophila*.

Author contributions: S.B.M.G., P.D.P., H.R., and K.V. designed research; S.B.M.G., P.D.P., and D.T. performed research; P.D.P., O.V.R., and S.P. contributed new reagents/analytic tools; S.B.M.G., P.D.P., H.R., and K.V. analyzed data; S.B.M.G., P.D.P., H.R., and K.V. wrote the paper; and K.V. mentored the other authors.

Reviewers: S.A.-T., Harvard Medical School; and C.-F.W., University of Iowa.

The authors declare no conflict of interest.

Data deposition: The algorithm used in this paper is available on GitHub (https://github.com/pushkarparanjpe/freewalk).

[1]S.B.M.G. and P.D.P. contributed equally to this work.

[2]To whom correspondence should be addressed. Email: vijay@ncbs.res.in.

This article contains supporting information online at www.pnas.org/lookup/suppl/doi:10.1073/pnas.1713869115/-/DCSupplemental.

Published online February 13, 2018.

controlling flexor–extensor alternation, in bilateral and intersegmental coordination, as well as in propagation and termination of motoneuron activity as shown in vertebrates (7, 9, 30, 31). In *Drosophila*, recent studies on larval stages have identified two types of inhibitory premotor interneurons that are involved in controlling the motor activity required for larval crawling (32, 33). Moreover, also in larvae, segmentally repeated GABAergic interneurons have been identified and implicated in the control of the peristaltic wave of activity that underlies larval crawling (34). However, in adult flies, the identity and functional circuit features of the premotor interneurons that control leg motoneuron activity are poorly understood, and virtually nothing is known about the role of inhibitory premotor interneurons in walking behavior.

Here we investigate the role of premotor inhibition in walking by selectively suppressing GABAergic input to leg motoneurons. For this, we first develop an algorithm for the automated analysis of leg movements to characterize the walking parameters of wild-type flies from high-speed video recordings. Using genetic reagents that allow selective labeling of leg motoneurons together with targeted RNAi knockdown of neurotransmitter receptors, we then interrogate the nature of their premotor neuronal input during walking by analyzing the walking parameters. Our findings indicate that knocking down the expression of the $GABA_A$ receptor Rdl (Resistance to Dieldrin) results in dramatically reduced walking speed as well as reduced step length and failure to achieve sustained leg extensions during locomotion. Genetically restricting the knockdown to the adult stage or to subsets of motoneurons gives qualitatively identical results—slower walking speeds, shortened step lengths, without a general loss of coordination. Altogether, these findings identify premotor inhibition of motoneurons as an important determinant of leg movement and resulting speed of walking in freely behaving *Drosophila*.

Results

Recording and Analysis of Leg Movements in Freely Walking Flies. As a prerequisite for investigating whether premotor inhibitory inputs are required for appropriate walking behavior in *Drosophila*, we developed an automated high-speed video recording and analysis technique. This technique made it possible to record the protraction (swing) and retraction (stance) phases of leg motion at high resolution of [2,500 μm (67.5 pixel)] for each leg in freely walking flies. To record leg movements of freely walking flies at high spatiotemporal resolution, flies were placed in a transparent Plexiglas arena and their locomotor behavior was recorded by an overhead high-speed video camera (Allied Vision Technologies) at 200 frames per second (fps) (Fig. 1*A*). The arena has a square-shaped flat central bottom of 20 mm width and 10 mm height surrounded by two opposing inclined (45°) surfaces and has Teflon-coated walls at a height of 30 mm to discourage climbing. Single flies with wings clipped were introduced into the arena and preferentially walked across the flat part of its bottom. The recording video camera was fitted with a lens of 10× magnification. Illumination was from below, resulting in high-contrast images (Fig. 1*B*). An automated recognition procedure was employed to extract the leg movements of the freely walking fly from the recorded video images; only linear walking sequences were selected. For this, thresholding based on light intensity differences was used to demarcate the fly torso; watershed filtering was employed to delimit head, thorax, and abdomen; and computation of a body axis orientation vector based on these three body parts was carried out (Fig. 1*C*). Subsequently, based on the dynamic changes of this vector, the fly's motion was transformed from the camera's frame of reference to an inertial reference frame (fly's frame of reference) (Fig. 1*D*). This provided a stable image of the fly suitable for autodetection and analysis of leg movements. Flies 3–4 days old starved for 2–3 h were used for recording.

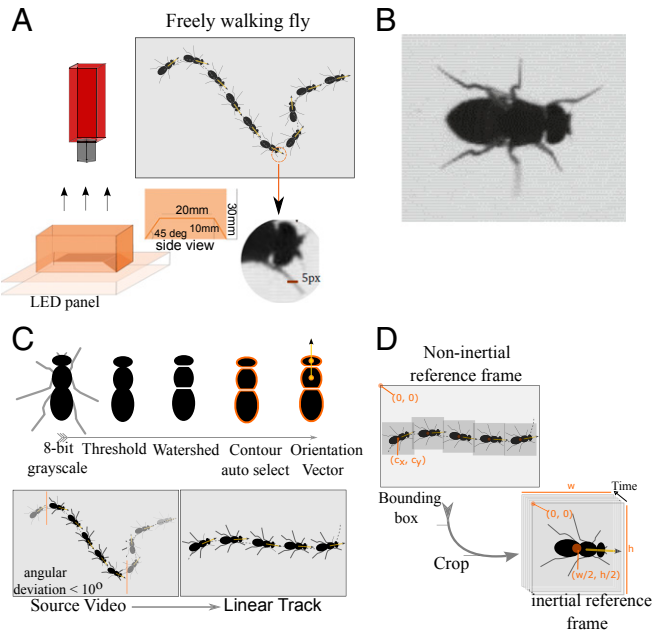

Fig. 1. Automated recording of walking behavior of freely moving flies. (*A*) Leg movements of freely walking flies were recorded with a 200-fps camera; flies were placed in the rectangular-shaped arena that has a square-shaped flat bottom of 20 mm width and 10 mm height with two opposing inclined (45°) surfaces and that is surrounded by teflon-coated walls at a height of 30 mm to discourage climbing; the arena is illuminated from below with an LED light source. (*B*) Dorsal view of the fly captured at a high resolution of 2,500 μm to 67.5 px. (Scale bar: 37 μm to 1 px.) (*C*) To obtain linear walking sequences, each frame is thresholded such that only the torso is visible. A watershed filter cuts the torso into three sections—the head, the thorax, and the abdomen. The centroids of the head and the body define the orientation vector. Enforcing a maximum angular deviation of 10° as a chief criterion, contiguous frames that constitute a linear walking bout are selected. (*D*) A minimum bounding box that encloses the fly body is used as a mask to crop each frame, and rotational transformation is applied so that the fly's linear motion occurs along the positive direction of the new *x* axis. The centroid of the fly was computed in each frame, and the origin of the new coordinated axis was shifted to the centroid. This transforms the non-inertial frame of reference to the inertial frame of reference such that the fly appears to be walking on a treadmill.

For a detailed characterization of these leg movement phases, an autodetection of leg movements from video frames was carried out, followed by the quantitative analysis of leg movements from the extracted leg-tip coordinate data. To autodetect the movement of all six legs in their entirety given the video frame of a fly, an algorithm was developed using an open source image analysis software package—Fiji (2013 lifeline version). The algorithm has been made accessible on GitHub (https://github.com/pushkarparanjpe/freewalk).

In this algorithm, light intensity thresholding was used to obtain a binary image of the fly, and its contour was autoselected as a full ROI (region of interest). Subsequently, the full ROI was adjusted such that legs were uncovered (torso ROI) and individual leg ROIs were computed by pixel-wise logical XOR between the full ROI and the torso ROI (Fig. 2*A*). (Alternatively, in simplified terms, this algorithm can be described according to binary morphological operations of erode and dilate as follows: erode the binary mask of the fly *n* times such that only the partially eroded torso remains, dilate the binary mask of the torso *n* times to restore the size of the torso, compute a third binary mask by performing a pixel-wise XOR operation between the full fly binary mask and the torso binary mask, obtain the binary mask of all six legs without the torso.)

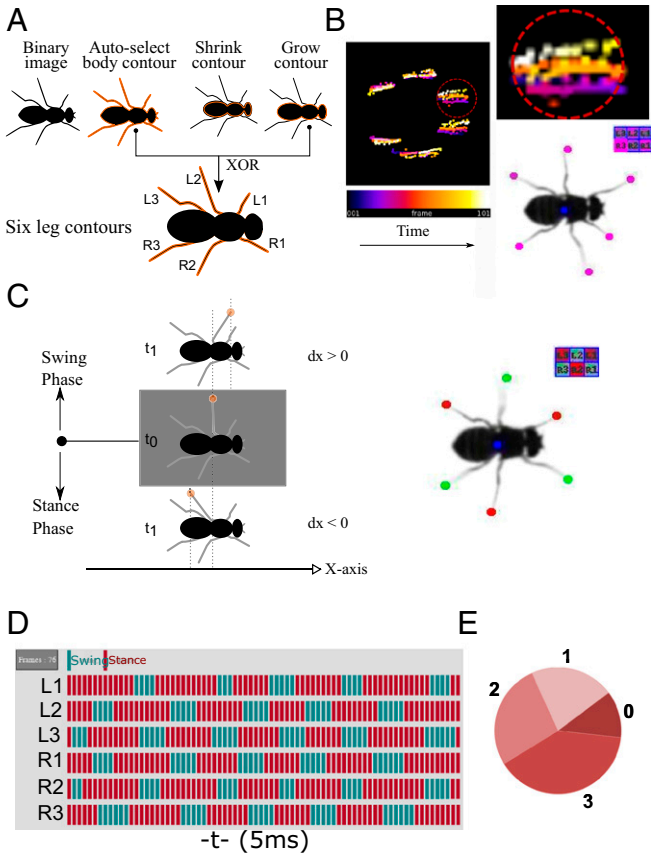

Fig. 2. Automated detection of leg movements in freely walking flies. (*A*) Fly body contour is autoselected and shrunk by 5 px. The contour selection is grown back by 5 px, as a result of which only the torso gets selected, leaving the legs out. The fly contour selection and the fly torso selection are combined through a XOR function. This gives a composite selection containing all six legs. (*B*) Temporal *z* projection of leg-tip trajectories allows rapid extraction of individual leg tips by drawing ROI selections around six clusters. The color-coded heat map with respect to time is a record of the trajectory of the leg tip during the entire walking bout and aids in demarcating adjacent legs. The darker the color, the more past it is, and the lighter the color, the more recent it is. The leg tips and the body centroid are annotated in every frame of the video to aid in assessing the quality of their detection. (*C*) Swing phase and stance phase classification are performed based on the sign of change in the *x* coordinate of the leg tip with respect to time. A positive change implies swing phase of the leg, while a negative change implies stance phase of the leg. A swinging leg was annotated by overlaying a green filled circle on its tip; a stancing leg was annotated by overlaying a red filled circle on its tip. No leg was annotated if it was stationary. In *Right*, the color-coded legs indicate the leg motion state. Red color indicates the leg stance phase, and green color indicates leg swing phase. (*D*) The swing, stance, or steady phase of each of the six legs with respect to time is represented as a series of colored ticks in a gait diagram. A representative gait diagram is shown in which each tick is 5 ms (-t- axis) in duration; red tick implies swing, and turquoise tick implies stance phase. (*E*) Three legs swinging concurrently defines a concurrency state of 3, two legs swinging concurrently defines a concurrency state of 2, one leg swinging alone defines a concurrency state of 1, while state 0 implies no leg was swinging.

After the leg's ROIs were isolated, the leg-tip coordinates were extracted for further analysis. A temporal projection of the leg-tip coordinates resulted in an image that consisted of six distinct clusters, which allowed efficient isolation and assignment of each leg-tip coordinate to the respective hemithoracic segment (Fig. 2*B*). The color-coded heat map is a temporal record of the trajectory of all of the legs during the entire walking sequence, and it aids in demarcating adjacent legs from each other. With respect to time, the heat map indicates the darker the color, the more in the past it is, and the lighter the color, the more recent it is. Each leg-tip coordinate was a 3-dimensional entity comprising x, y and frame number values. From these values, two distinct phases of leg motion could be identified—namely, the protraction (swing) phase in which the leg moves in a posterior to anterior direction, and the retraction (stance) phase in which the leg moves in an anterior to posterior direction (Fig. 2*C*). During the protraction (swing) phase, the leg is raised from the substrate and is moving in a posterior to anterior direction relative to the body; during the retraction (stance) phase, the leg is in contact with the substrate and is moving in an anterior to posterior direction relative to the body. The dynamics of swing/stance events for each of the six legs' time was represented in a diagram similar to the "gait diagram" traditionally used to visualize walking gaits (Fig. 2*D*). To indicate the degree of coordination between legs, concurrency scores were calculated and depicted in the concurrency score pie chart based on the number of events in which legs undergo the leg swing phase concurrently (Fig. 2*E*). The relationship between the concurrency scores and leg coordination corresponds to the degree of coordination between the legs; the higher the concurrency, the more legs swing together, and the lower the concurrency, the fewer legs swing together. When three legs swing together, the concurrency state is 3, corresponding to tripod coordination; when two legs swing together, the concurrency state is 2, corresponding to tetrapod coordination; and when one leg is in swing phase, the concurrency state is 1, corresponding to pentapod coordination. In coordinated walking flies at a given time, all three legs are in swing phase and the other concurrent legs are in stance phase, corresponding to tripod coordination, and in the pie chart, the occurrence of concurrency state 3 increases. In contrast, in uncoordinated walking flies, there is a decrease in the leg swing concurrency corresponding to either tetrapod or pentapod coordination, and in the pie chart, the occurrence of concurrency states 2 and 1 increases.

Characterization of Swing and Stance Phases in Freely Walking Flies. In an initial baseline behavioral analysis of freely walking flies, we used this technique to analyze the relationship between walking speed and leg protraction (swing) and retraction (stance) phase characteristics in the wild type. For this, we acquired ∼39 video recordings of flies walking freely in an arena. These video recordings were grouped into two classes with respect to walking speed. These classes are fast (21.0 mm/s to 34.0 mm/s) and slow (7.0 mm/s to 20.0 mm/s) (see Movie S1).

The range of speed of the flies walking was between 7 mm/s to 34 mm/s, and the represented average speed we observed was 25 mm/s, as reported earlier (20, 26). Approximately 20 mm/s were underrepresented data as mentioned in previous reports (26); we used this as the cutoff and grouped below 20 mm/s speed as slower walking flies and above 20 mm/s as faster walking flies. Of the 39 flies assayed, we observed that 40% of flies were "slow" and 60% of flies were "fast." Analysis of recorded leg movements indicated that faster walking flies protracted their legs farther (increased swing amplitude) than slower walking flies (Fig. 3*A*). Similarly, faster walking flies retracted their legs farther (increased stance amplitude) compared with slower walking flies (Fig. 3*C*). The largest difference in the length of protraction between the fastest walking group and the slowest walking group was ∼300 μm; this difference amounts to about one-third of the average body length of the animal. Faster walking flies completed their leg protractions more rapidly (decreased swing duration) than the slower walking groups (Fig. 3*B*). Faster walking flies also completed their leg retractions more rapidly (decreased stance duration) than the slower walking groups (Fig. 3*D*). The largest difference in the duration of retraction (stance duration) between the fastest and the slowest walking group was ∼30 ms. The fastest walking animals thus complete each metachronal

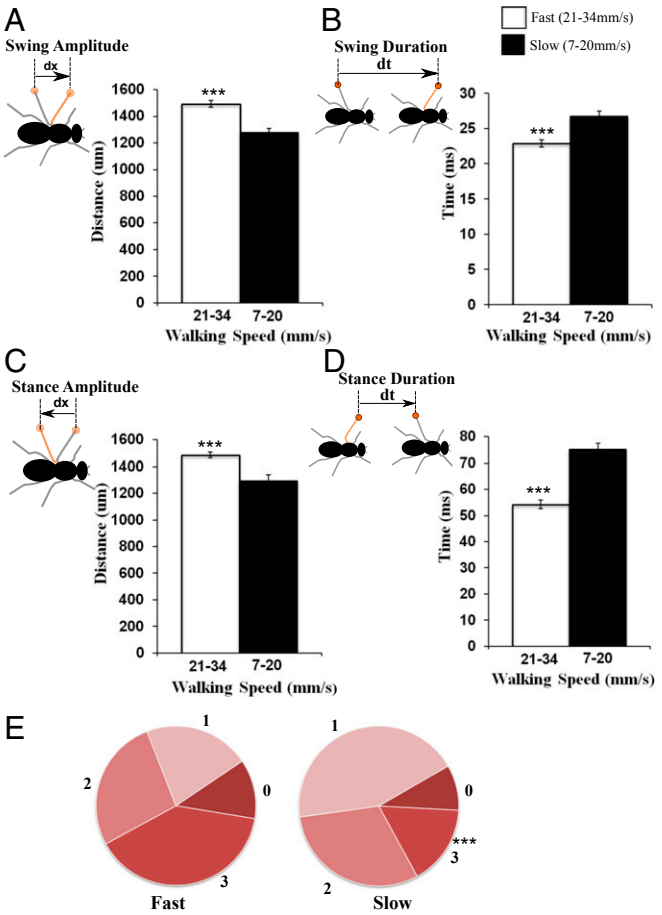

Fig. 3. Relationship between walking speed and leg phase characteristics in freely walking flies. Leg movement parameters are quantified and classified into two speed intervals: slow (7.0–20.0 mm/s) and fast (21.0–34.0 mm/s). (*A*) Swing amplitude is the average displacement of the leg tip during the swing phase as calculated in the fly's inertial reference frame; it increases as the walking speed increases. (*B*) Swing duration is the time of the swing phase; it decreases as the walking speed increases. (*C*) Stance amplitude is the average displacement of the leg tip during the stance phase as calculated in the fly's inertial reference frame; it increases as the walking speed increases. (*D*) Stance duration is the time of the stance phase; it decreases as the walking speed increases. (*E*) Concurrency state proportions change with respect to walking speed. State 3 is proportionately higher at faster walking speeds but lower at slower walking speeds. $n = 39$ videos. Quantitative analysis for the entire bar plots was performed using Student's t test. The entire bar plots represent mean ± SEM (***$P \leq 0.001$). Quantitative analysis for the pie chart was performed using two-way repeated measures (RM)-ANOVA and showed significant difference in the concurrency state 3 slower walking flies compared with fast walking flies, $F(3, 111) = 42.17$, $P < 0.001$. Post hoc testing using Sidak multicomparison test showed a significant difference in concurrency state 3 of slow walking flies in comparison with fast walking flies (***$P < 0.001$).

wave in ∼33% less time than the slowest walking animal. We also observed that the concurrency state proportions change with respect to walking speed. Concurrency state 3 corresponding to a tripod gait is proportionately more prevalent for faster walking flies than for slower walking flies (Fig. 3*E*). Overall these results quantify the way in which wild-type flies alter the length and duration of leg swing and stance phases as they modulate their walking speed.

To show our video assay is robust and as a positive control, we focused on the stumble gene known be involved in proprioceptive sensation and expressed in multidendritic sensory neurons (35); the corresponding *Drosophila* stumble mutant was reported to have uncoordinated walking behavior. Using the video analysis system, we were able to characterize the defective walking behavior in stumble mutants with uncoordinated walking as depicted in pie charts. We were also able to observe significant reduced walking speed and changes in leg motion parameters in these mutant flies (Fig. S2 and Movie S6).

Targeted Knockdown of Rdl Provides Evidence for GABAergic Premotor Inhibitory Input to Leg Motoneurons During Walking. To determine if premotor inhibition of leg motoneurons might be important for correct walking behavior, we conducted a screen for walking deficits caused by targeted knockdown of neurotransmitter receptors. For this, UAS-RNAi constructs for receptors of the neurotransmitters GABA, glutamate, and acetylcholine were used together with the OK371Gal4 driver, which targets UAS transgene expression to glutamatergic neurons and hence labels all leg motoneurons (Fig. 4*A*). Expression of OK371Gal4 is controlled by the enhancer of the *Drosophila* vesicular glutamate transporter gene, *VGLUT* (36).

Initial screening for walking deficits in these RNAi knockdown experiments was carried out using a soot assay of leg footprints (17, 37). In this prescreen, the targeted knockdown of the $GABA_A$ receptor Rdl resulted in a prominent walking phenotype characterized by shorter step lengths compared with controls (Fig. 4*B*). For a more extensive characterization of the walking behavior deficits that resulted from this targeted Rdl knockdown, we used our automated video analysis to characterize the relationship between walking speed and leg swing and stance phase characteristics in a quantitative manner. Analysis of the video data revealed that the Rdl knockdown flies had a markedly reduced walking speed compared with controls (Fig. 4*C*) (see Movie S2). Moreover, the amplitude of the leg swing phase and consequently that of the leg stance phase was markedly shorter compared with controls (Fig. 4 *D* and *E*). Swing phase duration was significantly higher than controls (Fig. 4*F*), but there was no change in the duration of stance phases (Fig. 4*G*). The concurrency state 3, in which three legs swing nearly simultaneously, was proportionally reduced compared with controls (Fig. 4*H*). Shorter average swing amplitudes in every metachronal walking wave markedly reduced the reach of the animal, thereby reducing the walking speed. (Data shown here are for the T2 leg segment as a representative of other leg segments.)

As a control for the general efficiency of the Rdl knockdown, the panneuronal Elav Gal4 driver was used to target the UAS-Rdl RNAi reporter to all neurons; however, this resulted in larval lethality. Adult stage restricted targeting of UAS-Rdl RNAi with the Elav Gal4 driver did not affect viability, and prominent reduction in the expression of Rdl in the VNC neuropile as assayed by immunocytochemistry was seen (Fig. S1).

Given that Rdl is an ionotropic inhibitory neurotransmitter receptor, these results suggest that normal wild type-like walking behavior requires inhibitory premotor input to leg motoneurons mediated by GABA acting through the Rdl receptor.

Adult-Specific Targeted Rdl Knockdown in Leg Motoneurons Results in Abnormal Walking Behavior. Suppression of inhibitory premotor input by constitutive knockdown of Rdl throughout all developmental stages could potentially impact the formation of the walking circuit. To rule out the possibility that developmental effects were responsible for the observed walking phenotypes, we refined our analysis by performing adult-specific knockdown of Rdl in leg motoneurons. For this, we used the temperature-sensitive Gal4 repressor, Gal80ts, together with OK371Gal4 to limit the effects of the targeted knockdown to adult stages. Flies were grown at 18 °C and shifted to 29 °C posteclosion (Fig. 5*A*; Gal80ts is active at 18 °C and is inactive at 29 °C).

Soot assay prints reveal that adult-specific targeted Rdl knockdown also caused walking behavior phenotypes characterized

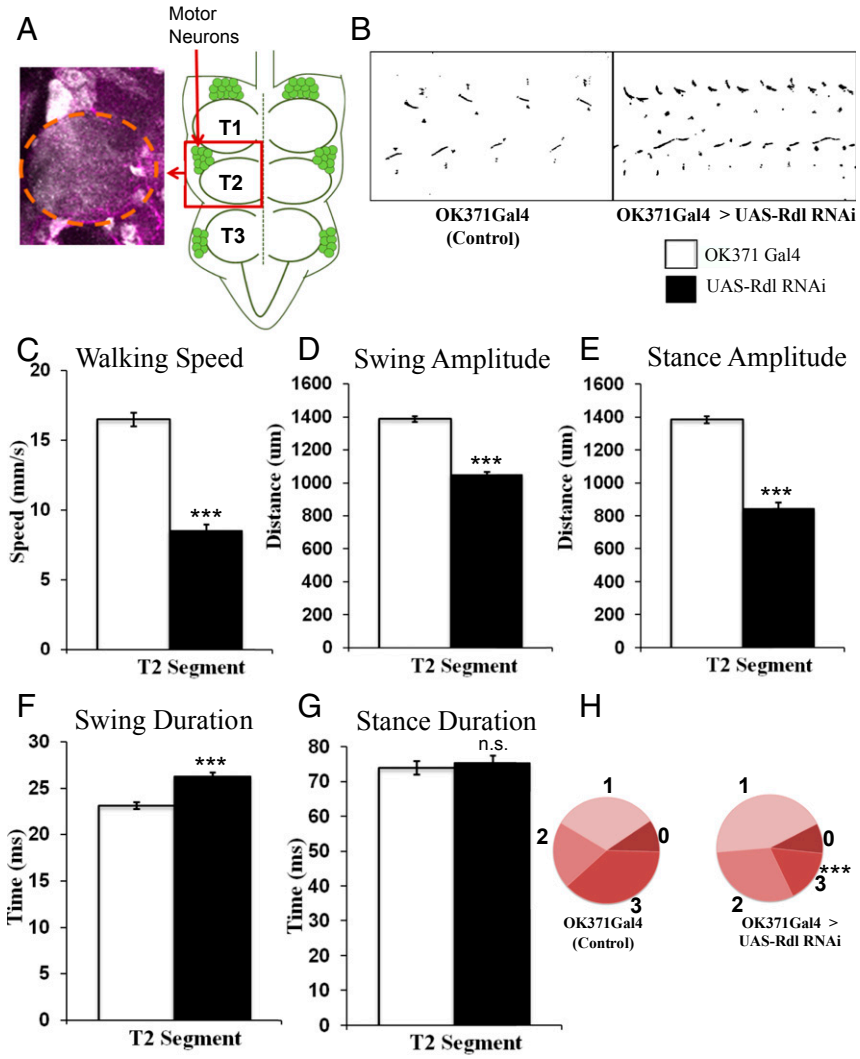

Fig. 4. Targeted knockdown of Rdl provides evidence for GABAergic inhibitory input to motoneurons in walking flies. (*A*) The OK371-GAL4 driver targets UASmCD8GFP expression to leg motoneurons. Schematic representation of motoneuron cell bodies localized in the VNC (*Right*). Enlarged T2 hemineuromere region showing GFP marked motor neuron cell bodies and dendritic arborization (*Left*). Orange circled region indicates neuropile. (*B*) Rdl receptor knockdown using OK371 GAL4 in all leg motoneurons results in shorter step length as revealed by the soot imprints. (*C*) Rdl receptor knockdown using OK371 GAL4 in all leg motoneurons results in a significant decrease in walking speed. In this and all subsequent figures, the left bar indicates control and the right bar indicates knockdown. (*D–F*) Rdl receptor knockdown using OK371 GAL4 in all leg motoneurons results in reduced amplitudes of swing and stance and increased swing duration. (*G*) Stance duration is unaffected. (*H*) Concurrency state 3 is significantly decreased by Rdl receptor knockdown. Left circle, control; right circle, knockdown. Controls (Dicer2; OK371 Gal4 > UAS-mCD8GFP) $n = 76$; experiment (Dicer2; OK371 Gal4 > UAS-Rdl RNAi) $n = 68$. n.s., not significant. Quantitative analysis for the entire bar plots was performed using Student's t test. All of the bar represents mean ± SEM (***$P \leq 0.001$). Quantitative analysis for the pie chart was performed using two-way repeated measures (RM)-ANOVA and showed significant difference in the concurrency state 3 of OK371 Gal4-driven Rdl knockdown flies, $F(3, 426) = 276$, $P < 0.001$. Post hoc testing using Sidak multicomparison test showed a significant difference in concurrency state 3 of Rdl receptor knockdown flies compared with OK371 Gal4 control flies (***$P < 0.001$).

by shorter step length compared with controls (Fig. 5*B*). More detailed quantitative characterization of the walking phenotypes using video analysis showed that these flies had a markedly reduced walking speed compared with controls (Fig. 5*C*) (see Movie S3). Moreover, the amplitude of the leg swing phase and consequently that of leg stance phase was markedly shorter compared with controls (Fig. 5 *D* and *E*), and the durations of swing and stance phases were significantly higher than in controls (Fig. 5 *F* and *G*). The concurrency state 3, in which three legs swing together (tripod gait), was proportionally reduced compared with controls (Fig. 5*H*). (Data shown here are for the T2 leg segment as a representative of other leg segments.)

These results indicate that abnormal walking behavior also results if GABAergic inhibitory premotor input to leg motoneurons acting through the Rdl receptor is impaired specifically in mature adult stages.

Leg Motoneuron Subset-Specific Knockdown of Rdl also Results in Abnormal Walking Behavior. In the previously mentioned experiments, the inhibitory $GABA_A$ receptor Rdl was down-regulated in all of the fly's motoneurons by the OK371 Gal4 driver. To determine if targeted knockdown of Rdl limited to only a subset of the leg motoneurons might also result in aberrant walking behavior, we took advantage of a generated VGN 1-Intron Reg-3Gal4 driver. This driver targets reporter gene expression to only a small subset of leg motoneurons that innervate the trdm, fedm, tidm, and tadm muscles of the leg (Fig. 6*A*). Soot assay print assays reveal that motoneuron subset-specific targeted Rdl knockdown also caused walking behavior phenotypes (Fig. 6*B*). Detailed

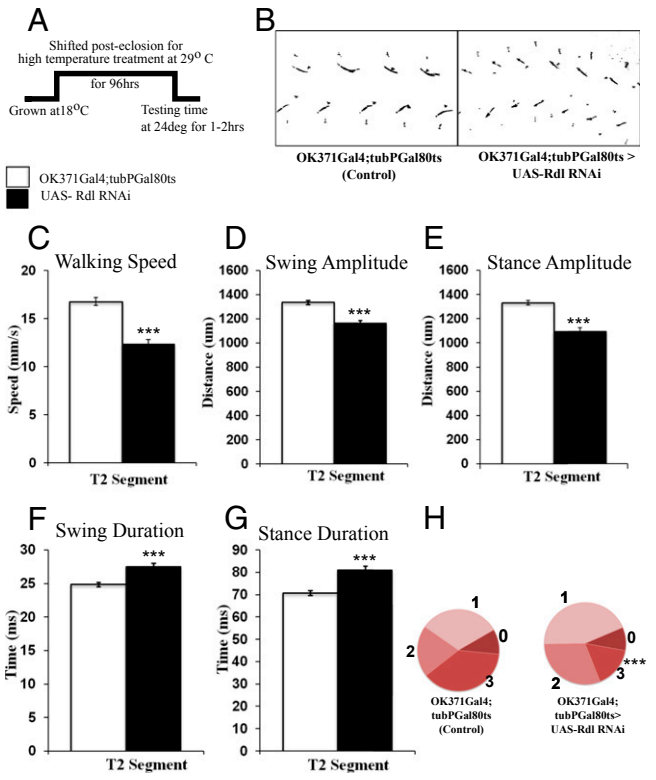

Fig. 5. Adult-specific Rdl knockdown in leg motoneurons results in abnormal walking behavior. (*A*) For adult-specific knockdown of the Rdl receptor, the GAL4 repressor Gal80ts was used to limit the effects to adult stages. For this, flies were grown at 18 °C and shifted to 29 °C posteclosion. The high-temperature treatment at 29 °C designed to knock down Rdl was held for 96 h. This was much longer than the reported half-life of the receptor turnover time of 32 h (46). The flies were then brought back to 24 °C for 1–2 h, during which time testing of walking behavior was carried out. (*B*) Adult-specific Rdl receptor knockdown using OK371 GAL4 in all leg motoneurons results in shortened step lengths, as shown in soot print images. (*C*) Rdl receptor knockdown flies show slower walking speed. In this and all subsequent figures, the left bar indicates control and the right bar indicates knockdown. (*D* and *E*) Amplitudes of swing and stance are shorter in Rdl knockdown flies compared with controls. (*F* and *G*) Swing and stance duration are increased longer in Rdl knockdown flies compared with controls. (*H*) Concurrency state 3 is significantly reduced in Rdl receptor knockdown flies. Left circle, control; right circle, knockdown. Controls (Dicer OK371Gal4; tubPGal80ts > UAS-mCD8GFP) $n = 108$; experiment (Dicer2; OK371 Gal4; tubPGal80ts > UAS-Rdl RNAi) $n = 77$. Quantitative analysis for the entire bar plots was performed using Student's *t* test. All of the bar represents mean ± SEM (***$P \leq 0.001$). Quantitative analysis for the pie chart was performed using two-way repeated measures (RM)-ANOVA and showed significant difference in the concurrency state 3 of adult-specific Rdl knockdown flies, $F(3, 549) = 109.7$, $P < 0.001$). Post hoc testing using Sidak multicomparison test showed a significant difference in concurrency state 3 of adult-specific Rdl receptor knockdown flies compared with OK371Gal4; tubPGal80ts control flies (***$P < 0.001$).

quantitative characterization of these walking phenotypes using video analysis showed that the flies had reduced walking speeds (Fig. 6*C*) (see Movie S4), and the amplitude of leg stance was markedly shorter, but no change in swing amplitude was observed (Fig. 6 *D* and *E*). The durations of leg swing and stance phases were significantly different compared with wild-type controls (Fig. 6 *F* and *G*). The concurrency state 3, in which three legs protract nearly simultaneously, was proportionally reduced compared with controls (Fig. 6*H*). The magnitude of the walking deficits caused by VGN 1-Intron Reg-3 Gal4–targeted Rdl knockdown in leg motoneuron subsets was generally smaller than that observed in OK371Gal4 targeted knockdown of Rdl in all leg motoneurons. (Data shown here are for the T2 leg segment as a representative of other leg segments.)

Nevertheless, these findings suggest that the suppression of premotor inhibitory input, even if it is limited to a small subset of leg motoneurons, is sufficient for perturbation of normal walking behavior.

Analysis of Rdl Knockdown in a Tsh-Gal80 Background Confirms Leg Motoneurons as Sites of Premotor Inhibition. The behavioral phenotypes caused by OK371Gal4 targeted knockdown of Rdl indicate that reduced GABAergic inhibition in the neurons genetically accessed by this Gal4 driver ("OK371 neurons") results in walking behavior deficits. Given that the leg motoneurons are prominent among the OK371 neurons, it seems likely that impairment of GABAergic inhibition of these motoneurons is responsible for the observed walking defects. However, the full complement of OK371 neurons as visualized by using OK371Gal4 to drive a UAS-GFP reporter includes numerous interneurons in the central brain and optic lobes, in addition to the leg motoneurons (Fig. 7*A*). Might impairment in the GABAergic inhibition of these central brain interneurons contribute to the walking defects observed in the OK371 targeted knockdown experiments?

To investigate this, we repeated the OK371Gal4-driven Rdl knockdown experiments in a Tsh-Gal80 background. Tsh-Gal80 does not affect the Gal4/UAS system in the central brain (38). However, it inhibits the Gal4/UAS system in all of the neurons of VNC, including motoneurons, as can be seen by using OK371Gal4 to drive a UAS-GFP reporter in a Tsh-Gal80 background (Fig. 7*B*). Soot print assays reveal that the walking pattern observed for the OK371-targeted Rdl knockdown animals in a Tsh-Gal80 background corresponds to that of wild-type controls (Fig. 7*D*); no walking deficits were apparent in the soot print assay. Quantitative characterization of these walking phenotypes using video analysis also showed that walking speeds (Fig. 7*E*) (see Movie S5), leg swing, and stance phases in these flies were not significantly different compared with wild-type controls (Fig. 7 *F*–*I*). Thus, no effects on walking were observed when OK371-targeted knockdown is limited to neurons in the central brain. (Data shown here are for the T2 leg segment as a representative of other leg segments.)

This finding strongly supports the notion that the behavioral phenotypes observed in OK371-Gal4–driven Rdl knockdown experiments is specifically due to the reduction of GABAergic inhibition in leg motoneurons and not in brain interneurons.

Discussion

In this report, we investigate the role of inhibitory premotor input to leg motoneurons in the walking behavior of freely moving *Drosophila* by suppression of GABAergic inhibitory input to leg motoneurons. Our findings indicate that the reduction of inhibitory GABAergic input to leg motoneurons caused by targeted Rdl down-regulation has marked effects on walking behavior. Thus, walking speed was markedly slower compared with controls, and correlated with this, the amplitudes of the leg protraction (swing) and retraction (stance) phases were significantly smaller and the durations of protraction (swing) and retraction (stance) phases were significantly higher than in controls. Moreover, the concurrency state, in which three legs swing together in a tripod gait, was proportionally reduced compared with controls. These prominent effects on walking parameters are similar regardless of whether Rdl down-regulation occurs throughout development or whether it is restricted to the adult stage. Taken together, these findings reveal a prominent, albeit highly specific role of GABAergic premotor inhibitory input to leg motoneurons in the control of normal walking behavior.

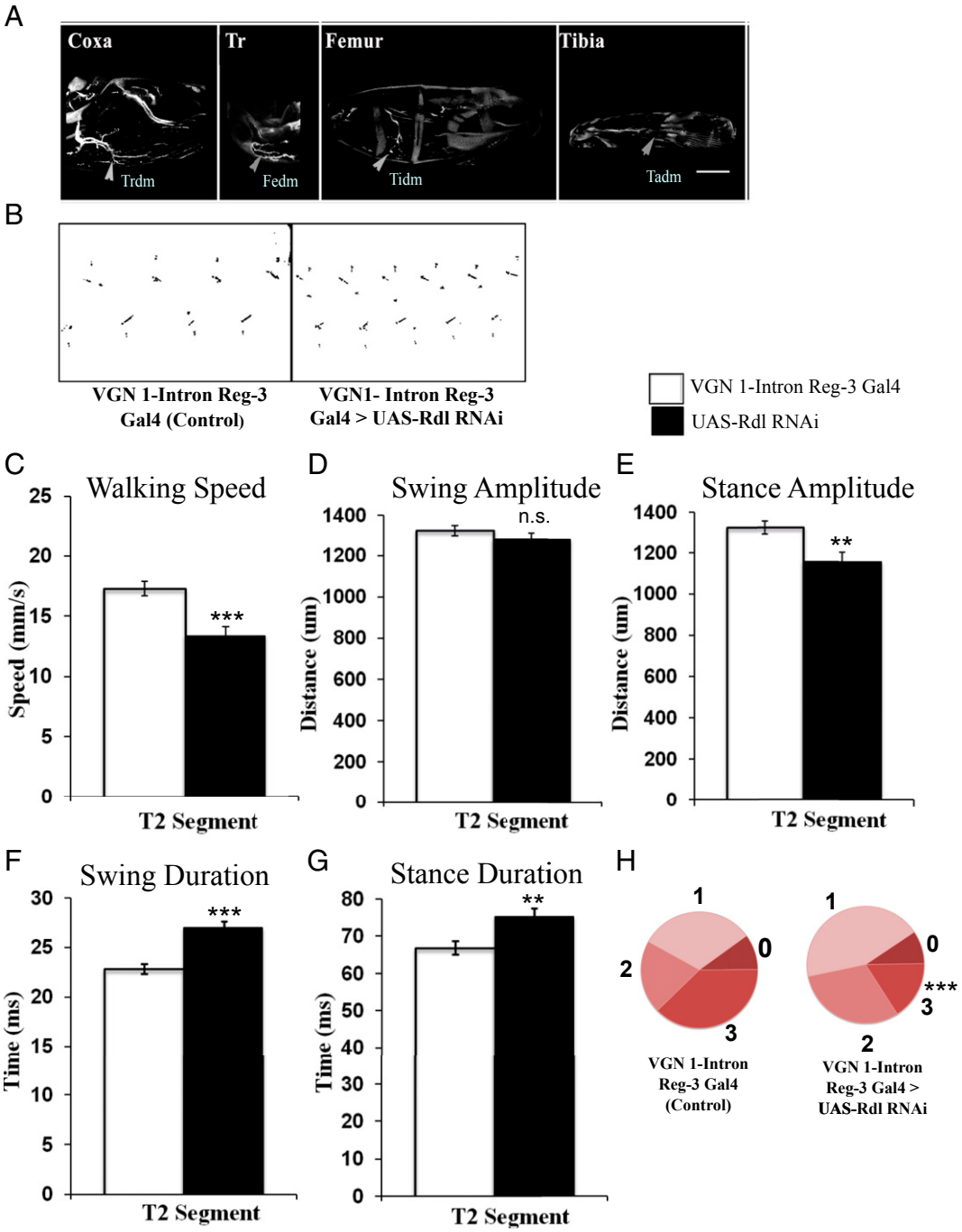

Fig. 6. Subset-specific knockdown of Rdl in leg motoneurons results in deficits in walking behavior. (*A*) Innervation patterns of leg motoneurons labeled by VGN 1-Intron Reg-3GAL4 driving UAS-GFP. (Scale bar: 50 μm.) Motoneuron axons innervating most of the depressor muscles (fedm, femur depressor muscle; tadm, tarsal depressor muscle; tidm, tibia depressor muscle; trdm, trochanter depressor muscle) are GFP labeled. (*B*) Motoneuron subset-specific Rdl receptor knockdown results in shortened step lengths as shown in the soot prints. (*C*) Rdl knockdown in subsets of leg motoneurons results in reduced walking speed. In this and all subsequent figures, the left bar indicates control and the right bar indicates knockdown. (*D* and *E*) Rdl knockdown in subsets of leg motoneurons results in decreased stance amplitude; swing amplitude is not affected. (*F* and *G*) Rdl knockdown in subsets of leg motoneurons results in longer swing duration and stance duration. (*H*) Concurrency state 3 is significantly reduced in Rdl receptor knockdown flies. Left circle, control; right circle, knockdown. Controls (VGN 1-Intron Reg-3 GAL4 > UASmCD8GFP) $n = 48$; experiment (VGN 1-Intron Reg-3 GAL4 > Dicer2; +; UAS-Rdl RNAi) $n = 45$. n.s., not significant. Quantitative analysis for the entire bar plots was performed using Student's *t* test. All of the bar represents mean ± SEM (**$P \leq 0.01$; ***$P \leq 0.001$). Quantitative analysis for the pie chart was performed using two-way repeated measures (RM)-ANOVA and showed a significant difference in the concurrency state 3 of subset-specific Rdl knockdown flies, $F(3, 270) = 133.4$, $P < 0.001$. Post hoc testing using Sidak multicomparison test showed significant difference in concurrency state 3 of subset-specific Rdl receptor knockdown flies compared with Vgn1Intron Reg-3 Gal4 control flies (***$P < 0.001$).

The insight into the role of premotor inhibition in walking control reported here is the result of two key experimental methodologies.

The first is the highly specific genetic access to identified neuronal populations that can now be attained in the *Drosophila* model system. This is made possible through remarkable targeted

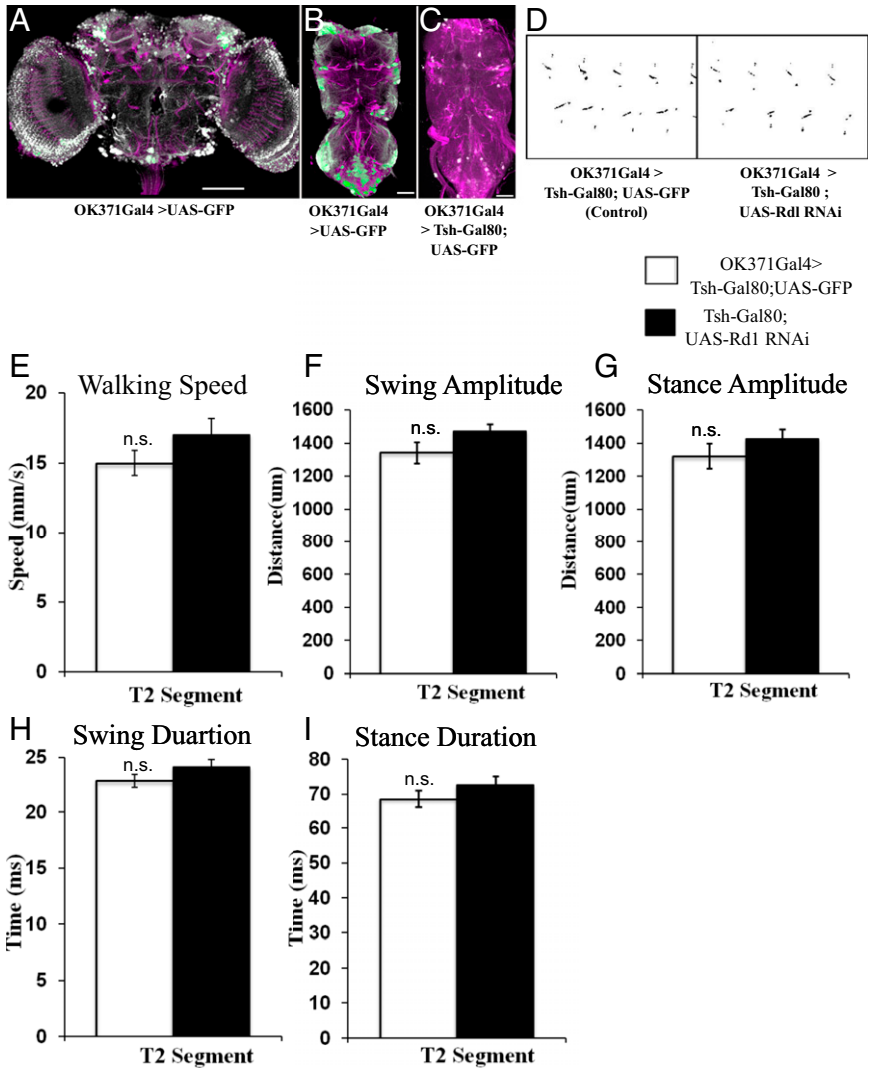

Fig. 7. Analysis of Rdl knockdown in Tsh-Gal80 background confirms leg motoneurons as sites of premotor inhibition. (*A*) OK371 Gal4-driven UAS-eGFP, which is expressed in motoneurons, is also expressed in numerous interneurons of the central brain and optic lobe. (*B*) OK371 Gal4-driven UAS-eGFP expression labels motoneurons in VNC. (*C*) Tsh-Gal80 inhibits the OK371Gal4 UAS-eGFP expression system in all VNC neurons including motoneurons. $n = 7$. (*D*) Behavioral analysis of OK371-driven Rdl knockdown in a Tsh-Gal80 background results in normal walking behavior as revealed in soot print images. (*E*) Rdl knockdown on walking behavior in Tsh-Gal80 background shows no change in walking speed compared with controls. In this and all subsequent figures, the left bar indicates control and the right bar indicates knockdown. (*F–I*) Amplitudes and durations of swing and stance are not affected in Rdl receptor knockdown animals using OK371 GAL4 in Tsh-Gal80 compared with wild-type controls. Controls (Dicer2; OK371Gal4 > Tsh-Gal80; UASGFP) $n = 30$; experiment (Dicer2; OK371Gal4 > Tsh-Gal80; UAS Rdl RNAi) $n = 30$. Quantitative analysis for the entire bar plots was performed using Student's *t* test. All of the bar represents mean ± SEM. n.s., not significant. (Scale bar: 100 μm in *A*, 50 μm in *B*, and 50 μm in *C*.)

expression systems, which together with the availability of libraries of genetically encoded drivers and reporters for molecular manipulation, make it possible to selectively up or down-regulate gene expression in highly specific neuronal populations in intact and freely behaving animals (11, 13, 39). In this study, we have used the Gal4/UAS expression system to achieve targeted genetic access to leg motoneurons and down-regulate GABAergic premotor input to these motoneurons by Rdl RNAi expression. In addition, we have utilized different forms of the Gal80 repressor to limit Gal4/UAS targeted expression to adult stages or to specific regions of the central nervous system and, hence, refine the spatiotemporal specificity of the resulting genetic access to motoneurons. Given the wealth of Gal4 drivers and UAS-RNAi reporters currently available, it will be possible to use similar transgenic technology to manipulate other inhibitory and excitatory neurotransmitter receptors in future studies of interneuronal components of the walking circuitry.

The second key method is the development of an advanced automated high-speed video recording and analysis technique that makes it possible to record the protraction (swing) and retraction (stance) phases at high spatiotemporal resolution for each leg in freely walking flies. With this technique, a quantitative assessment of leg motion parameters in freely walking animals can be carried out that can reveal subtle differences in amplitude and phase of movements of individual legs. This quantitative assessment has been critical for uncovering the role of premotor inhibition in walking behavior. Indeed, since the overall leg coordination during walking is unaffected by the reduction of GABAergic input to leg motoneurons, a more conventional qualitative behavioral analysis is unlikely to discern differences in walking between experimental and control animals. Recently, comparable high-resolution recording and analysis methods

have been used to quantify leg movement parameters in freely walking flies (25, 26, 40). These studies have provided important information on walking speed, interleg coordination, and other locomotor parameters and have also documented a role of sensory proprioceptive input to step precision during walking. The fact that these methods for high-resolution recording and analysis are currently available for studying leg movement parameters in freely walking flies should accelerate our understanding of walking behavior and of the neuronal circuitry involved in its control in *Drosophila*.

Given the prominent role of inhibitory premotor input to leg motoneurons reported here, it will now be important to identify and genetically access the premotor interneurons that provide this inhibitory input. While there is currently little information on the identity of the premotor interneurons that control the activity of leg motoneurons in adult flies, insight into inhibitory premotor interneurons has recently been obtained in larval stages. Thus, in *Drosophila* larva, a set of inhibitory local interneurons, termed PMSI neurons, have been identified that control the speed of axial locomotion by limiting the burst duration of motoneurons involved in peristaltic locomotion (32). Moreover, a second set of inhibitory premotor interneurons called GVLI neurons have been reported that may be part of a feedback inhibition system involved in terminating each of the waves of motor activity that underlie larval peristalsis (33). Finally, a pair of segmentally repeated GABAergic interneurons termed GDL neurons have been identified that are necessary for the coordinated propagation of peristaltic motor waves during both forward and backward crawling movements of larvae (34). Whether or not these inhibitory premotor interneurons persist into the adult stage and act in the control of walking behavior is not known. Glutamate has previously been suggested to act as an inhibitory neurotransmitter in the *Drosophila* CNS (41). To investigate the likelihood that centrally labeled OK371 nonmotoneurons might also play any role in the leg motoneuron inhibition studied here, we have carried out preliminary experiments involving knockdown of GluCl channels in motoneurons. These experiments reveal enhanced defects in walking behavior with loss of coordination, suggesting there could be a possible role of OK371-labeled glutamatergic interneurons in leg motoneuron inhibition.

In general terms, there are fundamental similarities in the principle mechanisms of locomotion in insects and vertebrates (e.g., ref. 3). These mechanistic similarities might also reflect similar motor circuit properties. For example, much like the PMSI neurons in *Drosophila*, which control the speed of locomotion by limiting motoneuron burst duration, the premotor V1 spinal interneurons in mammals are involved in the regulation of leg motoneuron burst and step cycle duration and thus also likely control the speed of walking movements (42). Hence, a characterization of the behavioral effects of inhibitory input to leg motoneurons in *Drosophila*, notably in freely walking flies, is likely to provide useful comparative information for understanding the functional role, and possibly the evolutionary origin, of premotor inhibition in vertebrate locomotory circuitry.

Material and Methods

The following fly strains were used: OK371-Gal4, UAS-dicer; OK371-Gal4, tubPGal80ts; UAS-dicer, OK371 Gal4, UAS-mCD8GFP; VGN 1-Intron Reg-3 Gal4; Elav-Gal4, +, tubPGal80ts; stumble - *stum*^{4487} (Bloomington); UAS-Rdl i8-10G RNAi (kind gift from Ron Davis, Scripps Research Institute, Jupiter, FL) (43); Tsh-Gal80, UAS-eGFp (37); and Tsh-Gal80, UAS-Rdl RNAi.

Generation of VGN 1-Intron Reg-3 Gal4 Transgenic Flies. The DVGlut regulatory region of 640 bp, corresponding to genome coordinates 2L:2403206–2403845 (release 6.16), was PCR-amplified from wild-type *Drosophila* melanogaster canton-s and cloned into restriction endonuclease enzyme sites EcoR1 and BamH1 of the pPTGal-attB vector (44) to generate VGN-Intron region3 Gal4.

Immunohistochemistry and Confocal Microscopy. Adult brain and thoracic ganglia (VNC) were dissected in phosphate buffer saline (PBS; pH 7.8) and fixed in 4% buffered formaldehyde for 45 min at 4 °C. Staining procedures were performed as previously described (17). Imaging of adult brain and thoracic ganglia were performed using the Olympus FV 1000 confocal microscope at 1-μm intervals. The imported *z* stack images were processed using FIJI and Adobe photoshop for further adjustments in brightness and contrast.

Immunostaining Protocol for Rdl Expression. The protocol was modified from the Yoshihisa Ozoe laboratory (45). Four-day-old male flies' thoracic ganaglia (VNC) were dissected on ice in PBS (pH 7.8) and fixed in 4% buffered formaldehyde for 1 h at 4 °C. The fixative was removed and was washed with PBS twice for 15–20 min followed by three washes with 0.3% PBTX (PBS + Triton X 100) for the duration of 1 h at 20-min intervals each at 4 °C. The tissues were further blocked in 10% NGS (goat serum) for 1–2 h. Further, the tissues were incubated in primary antibody diluted in 10% NGS and PBTX for the duration of 18 h at 4 °C. After the primary incubation, the tissues were washed with 0.3% PBTX for 1 h (three times for 20 min). Following the washes, the secondary antibody diluted in 10% NGS and PBTX was added for overnight. After secondary incubation, the tissues were washed with PBTX five times and mounted on glass slides using Vectashield (Vectar Laboratories) mounting media. Imaging of thoracic ganglia was performed using an Olympus FV 1000 confocal microscope at 1-μm intervals. The imported *z* stack images were processed using FIJI and Adobe photoshop for further adjustments in brightness and contrast.

Antibodies Used. The following primary antibodies were used: Chicken pAbα-GFP (1:1,000, Abcam), Rabbit (Rb) α-GFP (1:4,000, Abcam), mouse (ms) a-Neuroglian (BP104, 1:40; DSHB), Rabbit α- Rdl (1:500) (kind gift from Yoshihisa Ozoe, Shimane University, Matsue, Japan). The following secondary antibodies were used: Alexa fluor-488, -568, and -647 (1:400) from Invitrogen were used in all staining procedures.

ACKNOWLEDGMENTS. We acknowledge Avinash Khandelwal, Akila Sridar, and Swati Krishnan for their contribution in preliminary soot assay experiments; Sanjay Sane, Vatsala Thirumalai, Durafshan Sakeena, Dhananjay Chaturvedi, Krishan Badrinath, and Umashankar for their valuable suggestions and comments; and Ashutosh Shukla for helping in statistical analysis. We are thankful to Ron-Davis, the Vienna Drosophila Resource Center, the Bloomington Stock Centre, and the National Centre for Biological Sciences fly facility for generously providing the fly reagents. We also thank Central Imaging and Flow facilities for the Olympus FV1000 microscopes at NCBS. This work was supported by a J. C. Bose Fellowship (to K.V.).

1. Wilson DM (1966) Insect walking. *Annu Rev Entomol* 11:103–122.
2. Orlovsky GN, Deliagina TG, Grillner S (1999) *Neuronal Control of Locomotion: From Mollusc to Man*, Oxford Neuroscience Series (Oxford Univ Press, Oxford), pp 84–97.
3. Pearson KG (1993) Common principles of motor control in vertebrates and invertebrates. *Annu Rev Neurosci* 16:265–297.
4. Pearson K (2000) Motor systems. *Curr Opin Neurobiol* 10:649–654.
5. Marder E, Bucher D (2001) Central pattern generators and the control of rhythmic movements. *Curr Biol* 11:R986–R996.
6. Goulding M (2009) Circuits controlling vertebrate locomotion: Moving in a new direction. *Nat Rev Neurosci* 10:507–518.
7. Goulding M, Bourane S, Garcia-Campmany L, Dalet A, Koch S (2014) Inhibition downunder: An update from the spinal cord. *Curr Opin Neurobiol* 26:161–166.
8. MacKay-Lyons M (2002) Central pattern generation of locomotion: A review of the evidence. *Phys Ther* 82:69–83.
9. Kiehn O (2011) Development and functional organization of spinal locomotor circuits. *Curr Opin Neurobiol* 21:100–109.
10. Rybak IA, Dougherty KJ, Shevtsova NA (2015) Organization of the mammalian locomotor CPG: Review of computational model and circuit architectures based on genetically identified spinal interneurons(1,2,3). *eNeuro* 2:ENEURO.0069-15.2015.
11. Pfeiffer BD, et al. (2008) Tools for neuroanatomy and neurogenetics in Drosophila. *Proc Natl Acad Sci USA* 105:9715–9720.
12. Pfeiffer BD, et al. (2010) Refinement of tools for targeted gene expression in Drosophila. *Genetics* 186:735–755.
13. Venken KJT, Simpson JH, Bellen HJ (2011) Genetic manipulation of genes and cells in the nervous system of the fruit fly. *Neuron* 72:202–230.
14. Baek M, Mann RS (2009) Lineage and birth date specify motor neuron targeting and dendritic architecture in adult Drosophila. *J Neurosci* 29:6904–6916.
15. Brierley DJ, Blanc E, Reddy OV, Vijayraghavan K, Williams DW (2009) Dendritic targeting in the leg neuropil of Drosophila: The role of midline signalling molecules in generating a myotopic map. *PLoS Biol* 7:e1000199.
16. Brierley DJ, Rathore K, VijayRaghavan K, Williams DW (2012) Developmental origins and architecture of Drosophila leg motoneurons. *J Comp Neurol* 520:1629–1649.

17. Syed DS, Gowda SBM, Reddy OV, Reichert H, VijayRaghavan K (2016) Glial and neuronal semaphorin signaling instruct the development of a functional myotopic map for Drosophila walking. *eLife* 5:e11572.
18. Strauss R, Heisenberg M (1993) A higher control center of locomotor behavior in the Drosophila brain. *J Neurosci* 13:1852–1861.
19. Strauss R, Heisenberg M (1990) Coordination of legs during straight walking and turning in Drosophila melanogaster. *J Comp Physiol A Neuroethol Sens Neural Behav Physiol* 167:403–412.
20. Robie AA, Straw AD, Dickinson MH (2010) Object preference by walking fruit flies, Drosophila melanogaster, is mediated by vision and graviperception. *J Exp Biol* 213: 2494–2506.
21. Berni J, Pulver SR, Griffith LC, Bate M (2012) Autonomous circuitry for substrate exploration in freely moving Drosophila larvae. *Curr Biol* 22:1861–1870.
22. Yellman C, Tao H, He B, Hirsh J (1997) Conserved and sexually dimorphic behavioral responses to biogenic amines in decapitated Drosophila. *Proc Natl Acad Sci USA* 94: 4131–4136.
23. Büschges A, Akay T, Gabriel JP, Schmidt J (2008) Organizing network action for locomotion: Insights from studying insect walking. *Brain Res Brain Res Rev* 57:162–171.
24. Borgmann A, Büschges A (2015) Insect motor control: Methodological advances, descending control and inter-leg coordination on the move. *Curr Opin Neurobiol* 33: 8–15.
25. Wosnitza A, Bockemuhl T, Dubbert M, Scholz H, Buschges A (2012) Inter-leg coordination in the control of walking speed in Drosophila. *J Exp Biol* 216:480–491.
26. Mendes CS, Bartos I, Akay T, Márka S, Mann RS (2013) Quantification of gait parameters in freely walking wild type and sensory deprived Drosophila melanogaster. *eLife* 2:e00231.
27. Grillner S, Matsushima T (1991) The neural network underlying locomotion in lamprey—Synaptic and cellular mechanisms. *Neuron* 7:1–15.
28. Szczupak L (2014) Recurrent inhibition in motor systems, a comparative analysis. *J Physiol Paris* 108:148–154.
29. Pearlstein E, Watson AHD, Bévengut M, Cattaert D (1998) Inhibitory connections between antagonistic motor neurones of the crayfish walking legs. *J Comp Neurol* 399:241–254.
30. Grillner S (2006) Biological pattern generation: The cellular and computational logic of networks in motion. *Neuron* 52:751–766.
31. Nishimaru H, Kakizaki M (2009) The role of inhibitory neurotransmission in locomotor circuits of the developing mammalian spinal cord. *Acta Physiol (Oxf)* 197:83–97.
32. Kohsaka H, Takasu E, Morimoto T (2014) A group of segmental premotor interneurons regulates the speed of axial locomotion in Drosophila larvae. *Curr Biol* 24: 2632–2642.
33. Itakura Y, et al. (2015) Identification of inhibitory premotor interneurons activated at a late phase in a motor cycle during Drosophila larval locomotion. *PLoS One* 10: e0136660.
34. Fushiki A, et al. (2016) A circuit mechanism for the propagation of waves of muscle contraction in Drosophila. *eLife* 5:e13253.
35. Desai BS, Chadha A, Cook B (2014) The stum gene is essential for mechanical sensing in proprioceptive neurons. *Science* 343:1256–1259.
36. Mahr A, Aberle H (2006) The expression pattern of the Drosophila vesicular glutamate transporter: A marker protein for motoneurons and glutamatergic centers in the brain. *Gene Expr Patterns* 6:299–309.
37. Maqbool T, et al. (2006) Shaping leg muscles in Drosophila: Role of ladybird, a conserved regulator of appendicular myogenesis. *PLoS One* 1:e122.
38. Clyne JD, Miesenböck G (2008) Sex-specific control and tuning of the pattern generator for courtship song in Drosophila. *Cell* 133:354–363.
39. Manning L, et al. (2012) A resource for manipulating gene expression and analyzing cis-regulatory modules in the Drosophila CNS. *Cell Rep* 2:1002–1013.
40. Uhlmann V, Ramdya P, Delgado-Gonzalo R, Benton R, Unser M (2017) FlyLimbTracker: An active contour based approach for leg segment tracking in unmarked, freely behaving Drosophila. *PLoS One* 12:e0173433.
41. Liu WW, Wilson RI (2013) Glutamate is an inhibitory neurotransmitter in the Drosophila olfactory system. *Proc Natl Acad Sci USA* 110:10294–10299.
42. Gosgnach S, et al. (2006) V1 spinal neurons regulate the speed of vertebrate locomotor outputs. *Nature* 440:215–219.
43. Liu X, Krause WC, Davis RL (2007) GABAA receptor RDL inhibits Drosophila olfactory associative learning. *Neuron* 56:1090–1102.
44. Sadaf S, Reddy OV, Sane SP, Hasan G (2015) Neural control of wing coordination in flies. *Curr Biol* 25:80–86.
45. Kita T, Ozoe F, Azuma M, Ozoe Y (2013) Differential distribution of glutamate- and GABA-gated chloride channels in the housefly Musca domestica. *J Insect Physiol* 59: 887–893.
46. Lyons HR, Gibbs TT, Farb DH (2000) Turnover and down-regulation of GABA(A) receptor alpha1, beta2S, and gamma1 subunit mRNAs by neurons in culture. *J Neurochem* 74:1041–1048.